

Identifying Galactic Cosmic Ray Origins with Super-TIGER

G.A. deNolfo*, W.R. Binns[†], M.H. Israel[‡], E.R. Christian[‡], J.W. Mitchell[‡], T. Hams*, J.T. Link[§], M. Sasaki[¶], A.W. Labrador^{||}, R.A. Mewaldt^{||}, E.C. Stone^{||}, C.J. Waddington**, M.E. Wiedenbeck^{††}

* CRESST/UMBC/NASA/GSFC, Greenbelt, MD 20771 USA

[†] Washington University, St. Louis, MO 63130

[‡] NASA/GSFC, Greenbelt, MD 20771

[§] CRESST/USRA/NASA/GSFC, Greenbelt, MD 20771

[¶] CRESST/UMCP/NASA/GSFC, Greenbelt, MD 20771

^{||} California Institute of Technology, Pasadena, CA 91125

** University of Minnesota, Minneapolis, MN 55455

^{††} Jet Propulsion Laboratory, California Institute of Technology, Pasadena, CA 91109

Abstract. Super-TIGER (Super Trans-Iron Galactic Element Recorder) is a new long-duration balloon-borne instrument designed to test and clarify an emerging model of cosmic-ray origins and models for atomic processes by which nuclei are selected for acceleration. A sensitive test of the origin of cosmic rays is the measurement of ultra heavy elemental abundances ($Z \geq 30$). Super-TIGER is a large-area (5 m^2) instrument designed to measure the elements in the interval $30 \leq Z \leq 42$ with individual-element resolution and high statistical precision, and make exploratory measurements through $Z=60$. It will also measure with high statistical accuracy the energy spectra of the more abundant elements in the interval $14 \leq Z \leq 30$ at energies $0.8 \leq E \leq 10$ GeV/nucleon. These spectra will give a sensitive test of the hypothesis that microquasars or other sources could superpose spectral features on the otherwise smooth energy spectra previously measured with less statistical accuracy. Super-TIGER builds on the heritage of the smaller TIGER, which produced the first well-resolved measurements of elemental abundances of the elements ^{31}Ga , ^{32}Ge , and ^{34}Se . We present the Super-TIGER design, schedule, and progress to date, and discuss the relevance of UH measurements to cosmic-ray origins.

Keywords: GCR, refractory, volatile, OB associations

I. INTRODUCTION

Super-TIGER (Super Trans-Iron Galactic Element Recorder) is a new long-duration balloon-borne instrument designed to measure the elements of atomic number $30 \leq Z \leq 42$ with individual-element resolution and high statistical precision, and make exploratory measurements through $Z=56$. It will also measure with high statistical accuracy the energy spectra of the more abundant elements of $14 \leq Z \leq 30$ at energies $0.8 \leq E \leq 10$ GeV/nucleon. With an effective geometry factor of $2.5 \text{ m}^2\text{sr}$ (taking into account interaction losses within the instrument), Super-TIGER will make $\sim 10\times$

improvement in statistics over its predecessor, the Trans-Iron Galactic Element Recorder (TIGER). The first flight is scheduled from Antarctica in 2012 and a second flight planned in 2014. With nearly 60 days of data from two Antarctic flights, and with an effective geometry factor $\sim 6\times$ greater than TIGER, Super-TIGER will address important questions about galactic cosmic rays (GCR) including their origin, acceleration, and transport throughout the Galaxy.

Super-TIGER builds on the heritage of the smaller TIGER, successfully flown on two balloon flights from Antarctica in December of 2001 and 2003, yielding 50 days of data and producing the first well-resolved abundance measurements of ^{31}Ga , ^{32}Ge , and ^{34}Se , and an upper-limit on ^{33}As [18], [25], [24], [26]. The data indicate nearly equal abundances of Ge and Ga, which, together with the enrichment of the refractory elements by a factor of 3-4, suggest that GCRs originate from a source mixture of about 20% ejecta from Wolf-Rayet stars and core-collapse supernovae mixed with 80% interstellar material of solar system composition with an acceleration mechanism in which refractory elements are preferentially accelerated over volatiles [26], [20]. In addition, TIGER results identified a mass dependent behavior for the refractory elements that is not explained by the model of [10]. Testing such a mass-dependent model requires an instrument with a significant increase in statistics to quantify the abundances of the rare elements ^{36}Kr , ^{37}Rb , and ^{38}Sr .

It is believed that galactic cosmic rays (GCRs) derive their energy from supernovae or perhaps from pulsars, but there is less consensus on which acceleration processes are at play and what source material is being accelerated. However, recent TIGER measurements of GCR elemental abundances corroborate the conclusions drawn from earlier measurements [2], [3]. A picture is forming in which GCRs originate from within OB associations, regions within our Galaxy that contain young massive stars, and experience fractionation consistent with a preferential acceleration of elements found in interstellar grains (refractory) relative to those

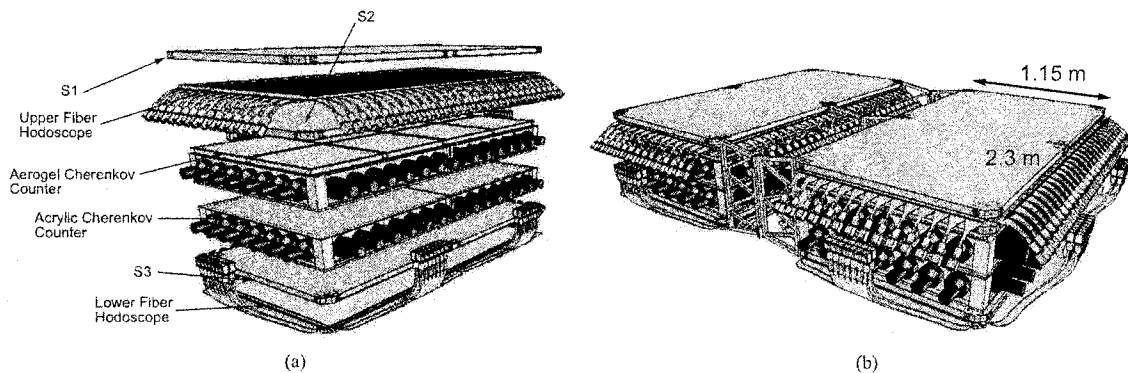


Fig. 1: (a) Exploded view of Super-TIGER instrument. (b) Full Super-TIGER concept (combining 2 modules together as shown in (a)).

elements found in the interstellar gas (volatile) [26], [20]. However, the interpretation of the TIGER data is limited by the lack of statistical precision owing to the limited number of events detected. A better test of this hypothesis requires a Super-TIGER. This is particularly true for the elements with $Z \geq 30$, where we expect enrichments from nucleosynthesis in massive stars.

Because the abundance ratio of secondary elements (produced by interstellar fragmentation of primaries, e.g. ^{33}As and ^{35}Br) to primary elements decreases with increasing energy above 1 GeV/nucleon, we expect variations of the UH element abundances with energy, which will help quantify the effects of cosmic ray transport through the interstellar medium. Super-TIGER will also measure the energy spectra of the more abundant elements of $14 \leq Z \leq 30$, permitting a sensitive test of the hypothesis that microquasars or other discrete objects could contribute to the otherwise smooth energy spectra previously measured with less statistical accuracy.

II. INSTRUMENT DESCRIPTION

Super-TIGER is based on the concept of combining 4 TIGER modules but with greater collecting power than four TIGER modules, because it allows cross-over events and more efficient use of the aerogel Cherenkov counter. From $30 \leq Z \leq 42$ Super-TIGER will achieve a statistical precision of $\sim 10\%$ or better for even-charges and $\sim 20\%$ or better for odd-charges. The instrument techniques used for charge and energy measurement are identical to those successfully demonstrated ([18], [21], [8], [9], [25], [24], [26]) on the smaller TIGER instrument with excellent Z-resolution ($\sigma_Z = 0.23$) in the $10 \leq Z \leq 38$ range.

The Super-TIGER instrument (Fig. 1a & 1b) consists of three planes of plastic-scintillator, two Cherenkov counters for velocity and charge measurements, and a scintillating fiber hodoscope for trajectory. Charges are measured on Super-TIGER using a combination of the dE/dx and Cherenkov detectors. The trajectory is

measured by the hodoscope, and is used to correct for the incidence angle and for instrument nonuniformities. For low-energy events, below the aerogel (C0) threshold, the sum of the top two scintillator signals (S1+S2), with a small velocity correction from the acrylic (C1) signal, will be used to determine charge. For high-energy events, the C1 signal, with a small correction from the C0 signal, will be used to identify charge. The S3 signal is used to identify and reject particles interacting in the instrument. The primary reasons for using two Cherenkov counters, each with different refractive indices in the TIGER experiment (2001 and 2003 flights), are to enable velocity corrections to the charge measurements, and to separate low energy from high energy nuclei, thus improving the charge identification, and to measure the energy spectra of the nuclei over the range $0.3 \leq E \leq 7$ GeV/nuc. The same method will be used for Super-TIGER, with the exception that the aerogel Cherenkov box will contain aerogel blocks with two different refractive indices ($n=1.04$ and 1.025), extending the energy range up to ~ 10 GeV/nuc.

The top scintillation layers (S1 & S2) that make the primary measurement of dE/dx are located just above and below the top hodoscope, respectively. The third scintillation counter (S3) is located just above the bottom fiber hodoscope and is used to identify particles that have interacted while traversing the detector stack. Each scintillator layer is composed of four individual modules, each of which contains a sheet of $1.16 \text{ m} \times 1.16 \text{ m} \times 0.8 \text{ cm}$ BICRON BC-416 plastic scintillator. The scintillation light is read out with four BC482A waveshifting bars placed around the perimeter of each sheet, with a single high-efficiency Hamamatsu RG7899-EGP PMT coupled to each end of each bar.

The Cherenkov light is collected using two light collection boxes. The first counter (C0) uses aerogel radiators. Each aerogel Cherenkov module includes four individual aerogel blocks mounted on top of a four-sectioned light-collection box. Three of the four modules will contain aerogel blocks of refractive index $n = 1.04$ (12 blocks total), while one module will contain four

blocks of index 1.025. These have thresholds of ~ 2.5 GeV/nuc and ~ 3.3 GeV/nuc, respectively. Thus, a total of 16 aerogel blocks of two indices are used for a total radiator area of 1.1 m x 4.4 m. The second counter (C1) uses an acrylic radiator (with Bis-MSB waveshifter added) with an index of refraction of ~ 1.5 , corresponding to a threshold-energy of ~ 0.3 GeV/nucleon. The acrylic radiator will consist of two 1x2 matrices of 1.16 m x 1.16 m modules, rather than a single large sheet.

Each of the two hodoscope planes consists of two perpendicular layers of square-cross-section fibers. Each fiber is a 1 mm square polystyrene scintillator (index of refraction 1.62) surrounded by 0.04 mm acrylic cladding. The fibers are formatted into tabs of six or seven fibers, so the effective segmentation of the hodoscope is ~ 6 -7 mm. The fibers at one end of each layer are split into ribbons of 8.9 cm length, with each group viewed by a single PMT (Hamamatsu R-1924). Thus there are a total of 13 PMTs for the full 116 cm width of fibers, giving a tube readout with coarse spatial resolution. On the far end (the fine spatial resolution end), each of the 8.9 cm length ribbons is subdivided into thirteen 7 mm tabs. The 13 tabs within each 8.9 cm ribbon are sequentially routed to the inputs of 13 PMTs, thus giving a finer spatial resolution that effectively acts as a vernier for the coarse tube readout. Each good event gives a hit at the fine end and one at the coarse end, thereby localizing the penetrating particle position to the 7 mm width of a fine fiber tab. The y-fibers are read out in a similar way. The tab size of 7 mm, which gives a root-mean-square deviation in position of $\sigma_{rms} = 7\text{mm}/\sqrt{12} = 2.0$ mm, was chosen to contribute only 0.01 to the overall charge resolution for $Z=40$ at the worst-case angle of incidence (45deg). The PMT signals are pulse height analyzed so that large signals from multiply charged nuclei can be readily distinguished from knock-on electrons. This method of reading out coded fibers has been shown to be highly effective for high-Z nuclei [25], [24].

III. EXPECTED PERFORMANCE

Brookhaven accelerator tests of NE-114 plastic scintillator show a charge resolution of 0.24 c.u. for silver nuclei, and by looking at interaction fragments from the ^{47}Ag , the response is linear in dE/dx over the charge range from ^{31}Ga through ^{47}Ag [1]. Therefore, we expect the good resolution in scintillation to continue at least into the Z range above 50. In the analysis of our TIGER data, we successfully modeled scintillator saturation (see also [28]) based on the detector response for iron and lower charges and extrapolated that to $Z \geq 30$. As part of the Super-TIGER program we plan to take a BC-416 scintillator detector to an accelerator facility (probably GSI in Darmstadt, Germany) and characterize its response to a fragmented Xe (or other appropriate charge that is available) beam for a several energies.

The Cherenkov counters should also achieve similar resolution values. In 1998 we calibrated an instrument

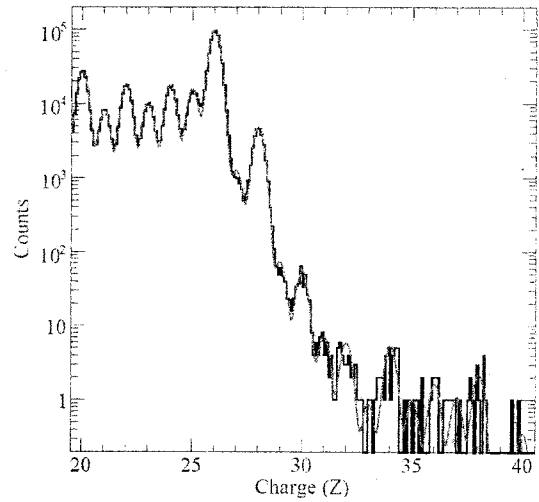


Fig. 2: Charge histograms from the combined results of the 2001 & 2003 TIGER flights. A maximum likelihood fit to the data is also shown (solid red curve).

complement, including the TIGER C0 (aerogel) and C1 (acrylic) Cherenkov counters, with a 10.6 GeV/nuc gold beam at Brookhaven National Laboratory [7]. In our Brookhaven calibration we obtained a resolution of 0.22 c.u. for gold nuclei in the acrylic counter, while in TIGER-2001 we achieved 0.23 cu resolution at iron for events above the aerogel Cherenkov threshold. The light collection of various Cherenkov counter configurations and radiators was modeled using a GEANT4 Monte Carlo (MC), which uses the measured optical properties of the reflector and PMT quantum efficiency, and Rayleigh scattering length in the Cherenkov radiator. Based on this simulation, we expect our charge resolution for high-energy nuclei will be essentially the same as for TIGER. Figure 2 shows the charge histograms from the combined results of both TIGER flights (50 days) which demonstrates the excellent charge resolution ($\sigma_Z = 0.23$ cu) we expect for Super-TIGER.

The Super-TIGER effective geometry factor (after interactions are removed) is $2.5 \text{ m}^2\text{sr}$ compared to $0.4 \text{ m}^2\text{sr}$ (calculated for ^{34}Se nuclei), for TIGER. The effect of solar modulation for flights in Dec. 2012 and 2014 compared to that during the TIGER flights in 2001 and 2003 gives an expected increase of a factor of 1.18 in numbers of particles. Additionally, assuming that Super-TIGER is flown twice for a total of 60 days compared to 50 days total flight time for TIGER gives an overall increase of nine for Super-TIGER over that of TIGER. In Fig. 3 we show a Monte Carlo of the numbers of nuclei expected in two flights assuming a total of 60 days at float and a charge resolution of 0.23 cu. There are clear peaks for each charge and we will be able to cleanly measure the abundances of all nuclei over the $Z=30$ -42 range.

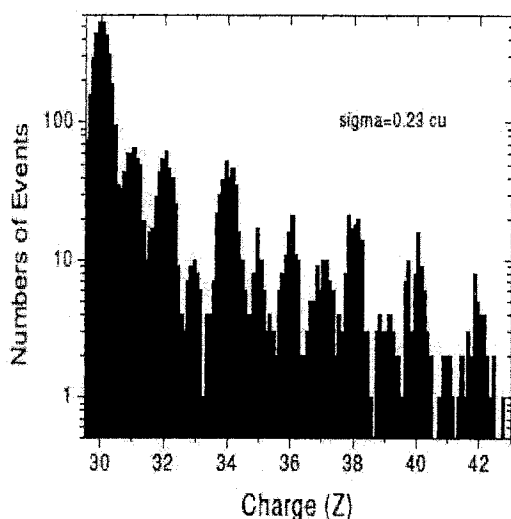


Fig. 3: Monte Carlo of expected numbers of events in 60 days for 0.23 cu resolution in charge.

IV. SUMMARY

Super-TIGER will make observations of the UH elements up to $Z=42$ with unprecedented statistical accuracy (and exploratory observations through $Z=60$), making it possible to probe all the aspects of cosmic ray history from the origin, to acceleration, and finally to propagation itself. In addition, the more abundant elements between $14 \leq Z \leq 30$ will be measured from 0.8 to 10.0 GeV/nuc, allowing for the possible identification of microquasar signatures. These results will provide an important feedback to the development of the Energetic Trans-Iron Composition Experiment (ENTICE), currently being studied as part of the Orbiting Astrophysical Spectrometer in Space (OASIS), one of the NASA Astrophysics Strategic Mission Concept Studies [6], [4]. ENTICE would have sufficient exposure and resolution to measure even the rarest individual elements including the actinides, ^{90}Th , ^{92}U , ^{94}Pu , and ^{96}Cm .

V. ACKNOWLEDGEMENTS

This research is supported by NASA under Grant number Super-TIGER NNX09AC17G.

REFERENCES

- [1] W.R. Binns, et al., 1991, Response of Scintillators to UH Nuclei, 22nd ICRC, 2, 511.
- [2] W.R. Binns, et al. 2001, in *AIP Conf. Proc. 589, Solar and Galactic Composition*, ed. R. F. Wimmer-Schweingruber (New York: AIP), 257
- [3] W.R. Binns, et al. 2005, *ApJ*, 634, 351
- [4] W.R. Binns, et al., 2009, Proceedings of the 31st ICRC (LODZ)
- [5] B. Byrnak, Lund, N., Rasmussen, L. II, Rotenberg, M., Engelmann, J., Goret, P., & Juliusson, E. 1983, Proc. 18th Int. Cosmic Ray Conf. (Bangalore), Vol. 2, 29
- [6] M. Christl, et al., 2009, Proceedings of the 31st ICRC (LODZ)
- [7] J.R. Cummings, et al. The Charge Identification Module (ZIM) for ACCESS: An Instrument Calibration using 10.6 GeV/nuc ^{79}Au , 26th ICRC, 5 (1999) 156.
- [8] G.A. DeNolfo, et al., 2005, Proc. 29th Int. Cosmic Ray Conf. (Pune), Vol. 3, 61
- [9] G.A. DeNolfo, et al., 2007, Proc. 30th Int. Cosmic Ray Conf. (Merida), Vol. 2, 43
- [10] D.C. Ellison, L.O'C. Drury, L., & L.P. Meyer, 1997, *ApJ*, 487, 197
- [11] S. Geier, et al. 2003, Proc. 28th Int. Cosmic Ray Conf. (Tsukuba), Vol. 6, 3261
- [12] S. Geier, et al. 2005, Proc. 29th Int. Cosmic Ray Conf. (Pune), Vol. 3, 93
- [13] J.C. Higdon, R.E. Lingenfelter, & R. Ramaty, 1998, *ApJ*, 509, L33
- [14] J.C. Higdon, & R.E. Lingenfelter, 2003, *ApJ*, 590, 822
- [15] D.J. Lawrence, et al. 1999, *Nucl. Instr. & Meth. Phys. Res. A*, 420, 402
- [16] R.E. Lingenfelter, R. Ramaty, & B. Kozlovsky, 1998, *ApJ*, 500, L153
- [17] R.E. Lingenfelter, & J.C. Higdon, 2007, *ApJ*, 660, 330
- [18] J.T. Link, 2003a, PhD dissertation, Washington University
- [19] J.T. Link, et al. 2001, Proc. 27th Int. Cosmic Ray Conf. (Hamburg), Vol. 6, 2143
- [20] J.T. Link, et al., 2009, Proceedings of the 31st ICRC (LODZ)
- [21] J.T. Link, et al. 2003b, Proc. 28th Int. Cosmic Ray Conf. (Tsukuba), Vol. 4, 1781
- [22] K. Lodders, 2003, *ApJ*, 591, 1220
- [23] J.P. Meyer, L.O'C. Drury, & D.C. Ellison, 1997, *ApJ*, 487, 182
- [24] B.F. Rauch, 2008, PhD dissertation, Washington University
- [25] B.F. Rauch, et al. 2007, Proc. 30th Int. Cosmic Ray Conf. (Merida), Vol. 2, 7
- [26] B.F. Rauch, et al., 2009, *ApJ*, 697, 2083-2088
- [27] S.H. Sposato, et al. 2000, in *AIP Conf. Proc. 528, Acceleration and Transport of Energetic Particles Observed in the Heliosphere*, ed. R. A. Mewaldt, J. R. Jokipii, M. A. Lee, E. Mobius, & T. H. Zurbuchen (New York: AIP), 433
- [28] G. Tarle, et al., 1979, Cosmic Ray Isotope Abundances from Chromium to Nickel, *ApJ*, 230, 607.
- [29] M.E. Wiedenbeck, & D.E. Greiner, 1981, *Phys. Rev. Lett.*, 46, 682
- [30] M.E. Wiedenbeck, et al. 2005, Proc. 29th Int. Cosmic Ray Conf. (Pune), Vol. 2, 277
- [31] M.E. Wiedenbeck, et al. 2007, *Space Sci. Rev.*, 130, 415
- [32] S.E. Woosley, & A. Heger, 2007, *Phys. Rep.*, 442, 269